

Highlights from the 17-Year Heavy Ion Program at the PHENIX Experiment at RHIC

John C. Hill
for the PHENIX Collaboration

Department of Physics and Astronomy, Iowa State University, Ames, IA 50011, USA

Abstract

A review is given of evidence from particle yields, elliptic flow and temperature measurements that a Quark Gluon Plasma (QGP) has been formed in relativistic collisions of heavy Au + Au nuclei. PHENIX studies of $d + \text{Au}$ and $^3\text{He} + \text{Au}$ collisions at 200 GeV/A were carried out to see if such correlations persist at lower energies compared to those at the LHC. Data from Au + Au collisions collected during the beam energy scan (BES) were used to determine both quark and nucleon number scaling. The HBT method was used to determine radii of the nuclear fireball at kinetic freeze out. Implications for the nuclear Equation of State (EoS) are discussed. After taking data starting in the year 2000 PHENIX was shut down in 2016. Plans for its successor named sPHENIX will be briefly discussed.

Keywords: *RHIC; PHENIX; nuclear modification factor R_{AA} ; elliptic flow; QGP temperature; $d + \text{Au}$; $^3\text{He} + \text{Au}$; HBT; sPHENIX*

1 Introduction

The Relativistic Heavy Ion Collider (RHIC) was built at Brookhaven National Laboratory (BNL) and collisions of beams of 130 GeV/A Au nuclei were observed in June 2000. PHENIX and STAR are two large detector systems built to study these collisions. In the summer of 2001 experiments with collisions of Au beams at the full RHIC energy of 200 GeV/A were studied. After extensive analysis of the results of runs from the years 2000 to 2004 a white paper [1] was published where evidence was given for the production of a Quark Gluon Plasma (QGP). The plasma was designated sQGP in illusion to the strong coupling observed. In addition the sQGP behaved not as a gas as many expected but like a liquid with almost zero viscosity, the so called “perfect liquid”. In 2010 the collisions of Pb nuclei were observed at the Large Hadron Collider (LHC) at a much higher energy density than at RHIC. This talk first discusses the suppression of particles in the hot dense nuclear medium created at RHIC which gives evidence that the QGP is strongly coupled. Next evident for flow of the QGP indicates that the plasma acts like a liquid rather than a

Proceedings of the International Conference ‘Nuclear Theory in the Supercomputing Era — 2016’ (NTSE-2016), Khabarovsk, Russia, September 19–23, 2016. Eds. A. M. Shirokov and A. I. Mazur. Pacific National University, Khabarovsk, Russia, 2018, p. 246.

<http://www.ntse-2016.khb.ru/Proc/Hill.pdf>.

gas. A description of recent measurements at PHENIX to measure the temperature of the QGP are presented. Results of measurements made at RHIC on $d + \text{Au}$ and $^3\text{He} + \text{Au}$ systems to determine if long-range correlations exist in small systems will be presented. Results of the low energy scan of $\text{Au} + \text{Au}$ collisions and HBT measurements of the radius of the nuclear fireball at freeze out will be given. Finally a short discussion of future experiments possible with the upgrade of PHENIX entitled sPHENIX will be presented followed by the conclusions.

2 Particle suppression in the QGP

In order to produce a QGP you need not only high energies but large volumes (times of the order of magnitude of 10 fm/c and 3–10 times normal nuclear density). This is necessary to sustain high energy densities and temperatures for an adequately long period of time. In the initial collision products of hard scattering are created followed by the creation of large numbers of quarks and gluons out of the vacuum resulting in a dense partonic medium. This medium can initially be the QGP but as it cools and expands it evolves into a hadronic gas. For 200 GeV/A Au collisions of the order of 10^4 particles are created. In order to study the properties of the QGP, particles that traverse the hot dense medium serve as a probe of its properties. For these studies of the properties of the medium we introduce a Nuclear Modification Factor R_{AA} .

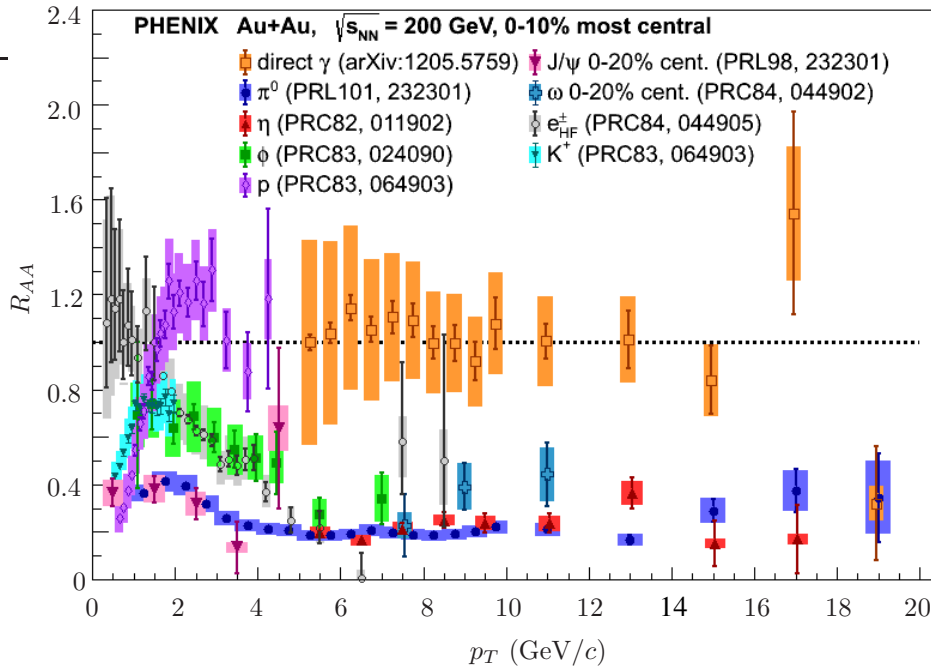


Figure 1: Plots showing R_{AA} for the 0 to 10 percent most central 200 GeV/A $\text{Au} + \text{Au}$ collisions for a wide variety of mesons, protons and direct photons at particle transverse momenta up to 19 GeV/c. Note the large suppression of hadrons but not direct photons.

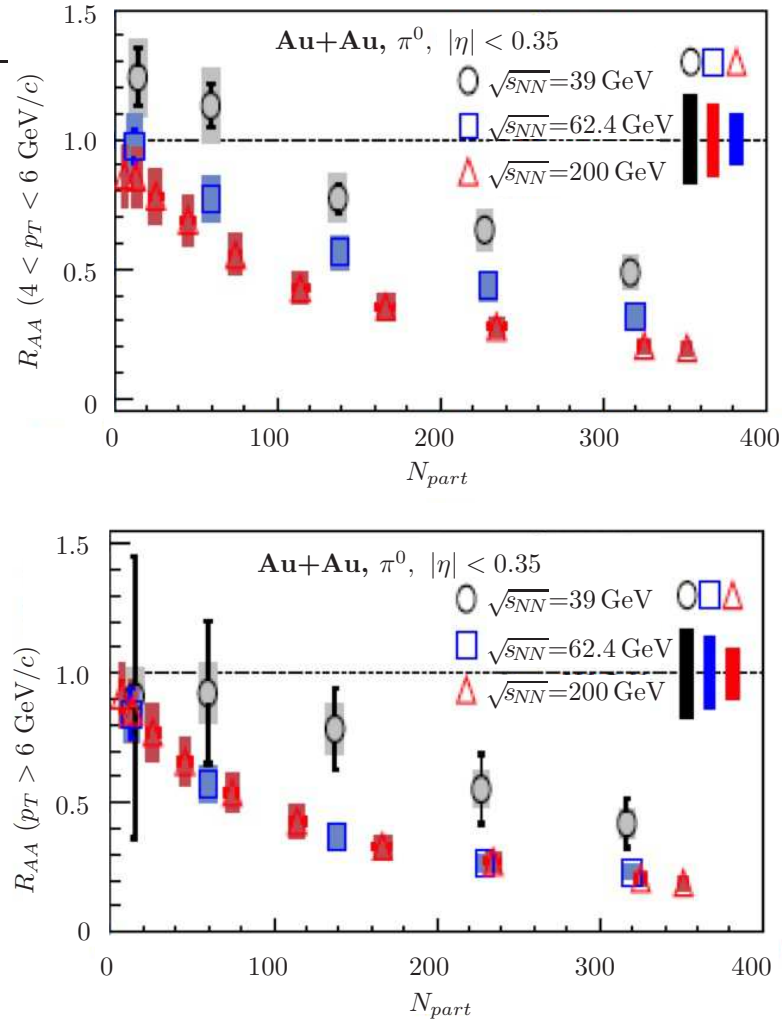


Figure 2: R_{AA} results for π^0 mesons for collision energies of 62.4 and 39 GeV/A. Particle numbers from 0 to 400 indicate a range from the most central to the most peripheral collisions.

In this factor the yield in nucleus-nucleus collisions is divided by the yield in $p + p$ collisions but scaled by the appropriate number of binary collisions N_{coll} which is calculated using the Glauber model. We do not expect to produce the QGP in $p + p$ collisions. Thus if the particles are not suppressed by the medium we expect $R_{AA} = 1.0$. A large number of measurements have been carried out at PHENIX to measure the response of various particles to passage through the hot dense medium created in Au + Au collisions. Using both Au + Au and $p + p$ data measured at PHENIX, R_{AA} for a number of different particles has been measured and the results are shown in Fig. 1 from the 2005 white paper [1]. Particularly striking is the large suppression of π^0 mesons [2] all the way out to 19 GeV/c. In addition large suppression of η [3] and ω mesons [4] was observed. This is an evidence for a strong suppression of mesons

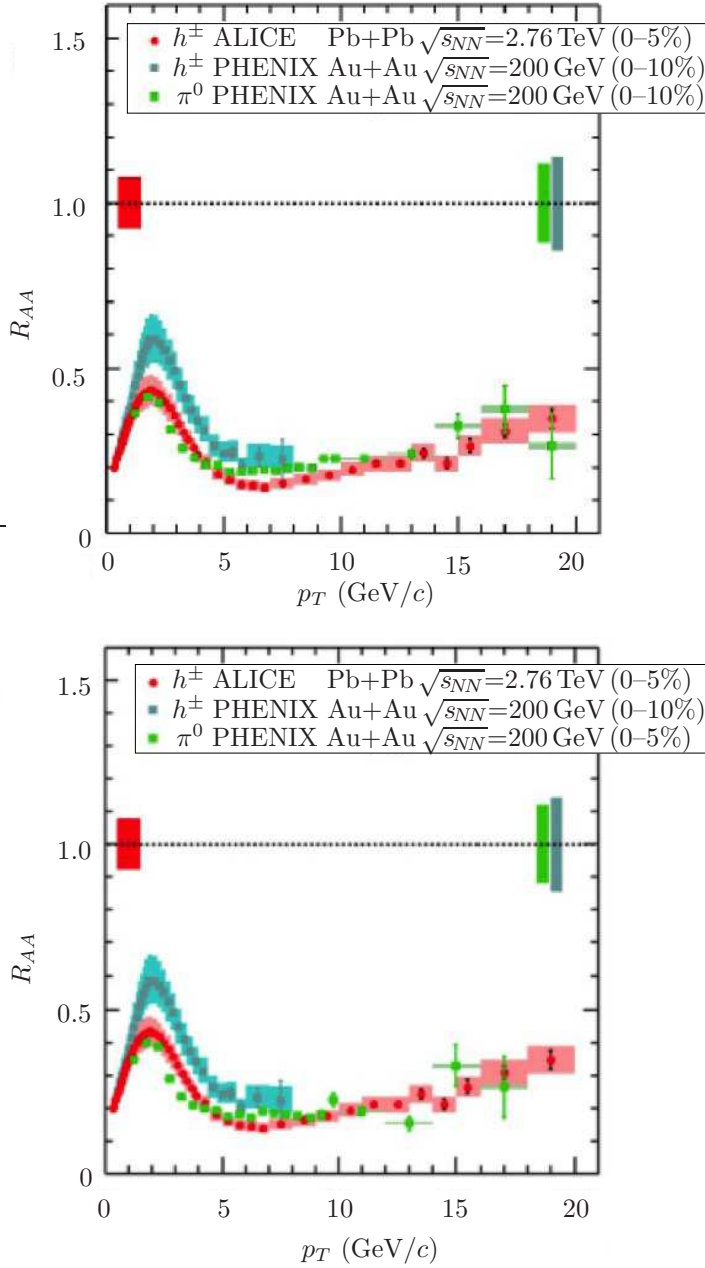


Figure 3: Plot showing R_{AA} for 200 GeV/A Au + Au collisions at PHENIX and 2.76 TeV/A Pb + Pb collisions at ALICE.

composed of the light u and d quarks in the sQGP.

The suppression of ϕ and K^+ mesons that contain a heavy s quark was measured. The suppression was less but still [5] significantly below an R_{AA} of 1.0 [5]. It might be expected that photons produced in direct interactions with the colliding quarks and gluons would not be suppressed by the sQGP since they only interact electromagnetically with the hot dense medium. This can be seen in the results in Fig. 1 for direct photons [6] where their R_{AA} is 1.0 within the error. We conclude that the sQGP

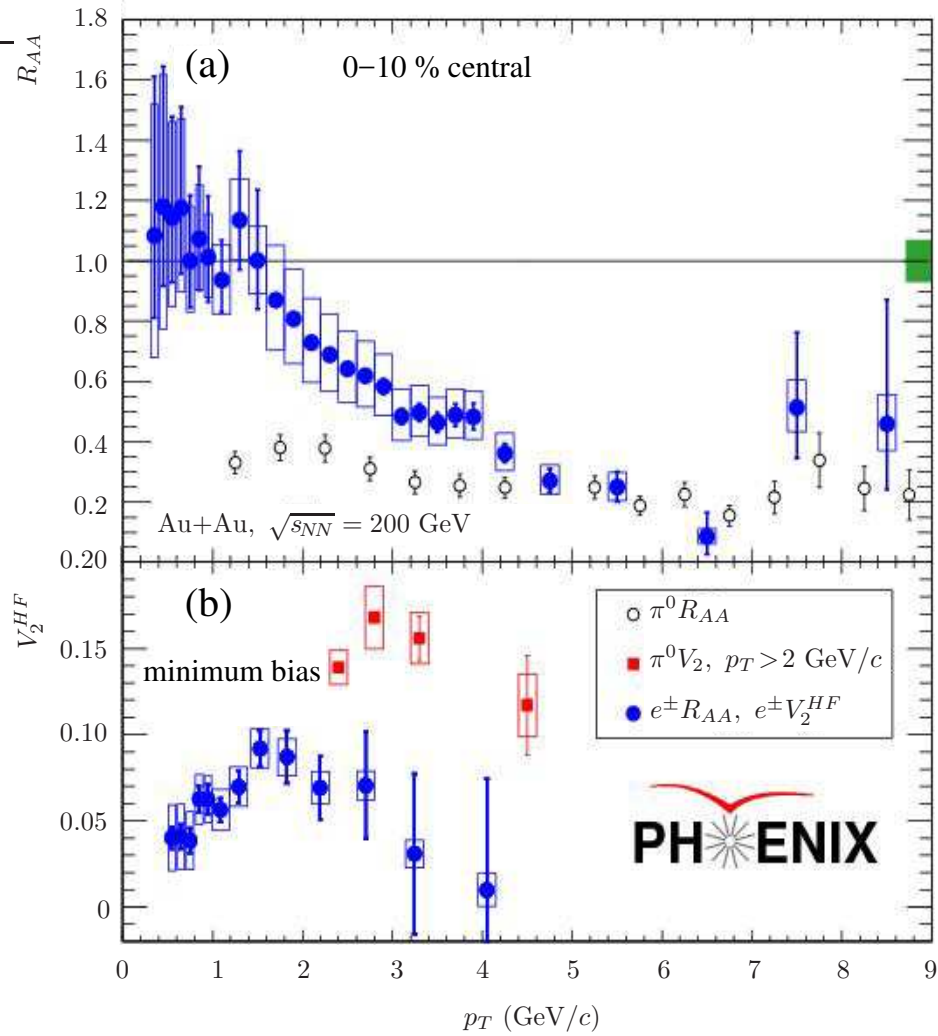


Figure 4: Plots of R_{AA} and v_2 in parts (a) and (b), respectively, for electrons from the decay of open charm and beauty. The data is for Au + Au collisions at 200 GeV and the 10 percent most central collisions.

strongly suppresses mesons made up of light u and d quarks but also significantly suppresses mesons composed of a heavier s quark. As expected direct photons are not significantly suppressed by the sQGP.

An important question is how does suppression in the sQGP change if we reduce the collision energy or the centrality of the collision. We would thus expect less suppression both for lower collision energy and more peripheral collisions. The Au + Au collisions were studied at 39 and 62.4 GeV/A and the results are compared with those at 200 GeV/A in Fig. 2. The suppression for a collision energy of 62.4 GeV/A is very similar to that for 200 GeV/A except that the suppression is slightly lower at 62.4 GeV/A for π^0 momenta below 6 GeV/c. By contrast when the collision energy is lowered to 39 GeV/A the π^0 is still suppressed but to a lesser extent than

at 62.4 GeV/A. It would be of interest to determine how far can we go down in collision energy and still see suppression. The data in Fig. 2 also shows that π^0 suppression is still large at all three collision energies [7] down to peripheral collisions where of the order of 50 particles are emitted.

The LHC has produced Pb + Pb collisions with an energy of 2.76 TeV/A. R_{AA} for the production of charged hadrons was measured with the ALICE detector. These results for R_{AA} are compared with those from Au + Au collisions at PHENIX [8] at a collision energy of 200 GeV/A in Fig. 3. From the figure it is observed that there is very little change in the suppression of the charged hadrons even though the collision energies at ALICE are much greater. One might expect a higher suppression due to the greater energy densities at ALICE but many more particles are produced so the recombination must be taken into account.

The suppression of u , d and s quarks in the sQGP is significant so it is interesting to test to what extent the much heavier c and b quarks are suppressed. To study this the R_{AA} for Au + Au collisions at 200 GeV/A was measured for electrons and positrons from decay of open charm and beauty. The R_{AA} for these particles is shown in the top part of Fig. 4 and compared [9] with results from π^0 . For the most central collisions electrons with p_T greater than 2.0 GeV/c are significantly suppressed.

From the study of the hot dense medium produced in Au + Au collisions at RHIC we can conclude the following:

1. In Au + Au collisions we have created a color opaque medium called the sQGP. The evidence is an observation of nuclear modification factors $R_{AA} < 1.0$.
2. Suppression of particles in the medium is prominent for collision energies down to 39 GeV/A.
3. The level of suppression at the higher energy densities at the LHC is similar to that at RHIC.
4. The level of suppression is still very significant for the heavy c and b quarks.

3 Evidence for flow in the QGP

A critical aspect of the establishment of the nature of the QGP has been the observation that the hot dense matter created in relativistic heavy ion collisions flows. The geometry of flow is illustrated in Fig. 5.

In studying the flow the following points are relevant.

1. The reaction geometry produces an almond shaped interaction region.
2. The compression of mass in the center produces an anisotropic p_T distribution.
3. The resulting p_T distribution is described in terms of $[1 + \sum_{n=1}^{\infty} 2v_n \cos[n(\phi - \Psi_R)]]$.
4. A finite v_2 is termed the elliptic flow. Ψ is in the plane of the beam and the impact parameter.

Flow data [8] for v_2 for collisions of Au + Au from PHENIX along with data from the much higher Pb + Pb collisions at the LHC is shown in Fig. 6. The values of v_2

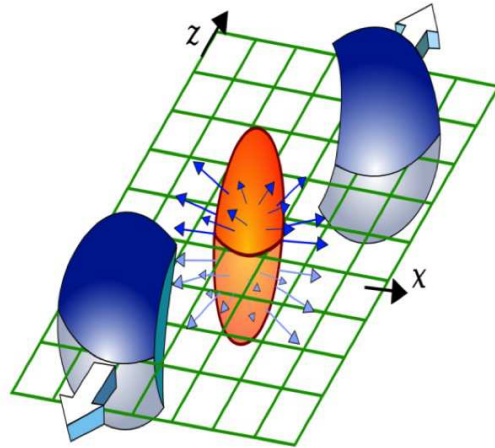


Figure 5: Diagram showing the geometry of flow for collisions of heavy nuclei.

show that flow is a prominent feature of Au+Au collisions. Relativistic hydrodynamic calculations [9] are a good fit to the data for $p_T < 2.0$ GeV/ c . A saturation of v_2 occurs as the energy reaches the RHIC regime. At saturation the QGP reaches the maximum achievable collective flow predicted by ideal hydrodynamics and the medium behaves as a nearly perfect fluid with very low viscosity. The ratio of shear viscosity to entropy density is very near the quantum lower bound. The data in Fig. 6 indicates that the fluid produced at LHC energies is very similar to that at RHIC. Evidently a much higher energy density is needed to create the QGP as a gas.

The quark scaling is an important signal indicating that a QGP has been formed. In Fig. 7 v_2 vs $m_T - m_0$ is plotted on the upper panel for a number of mesons ($n_q = 2$)

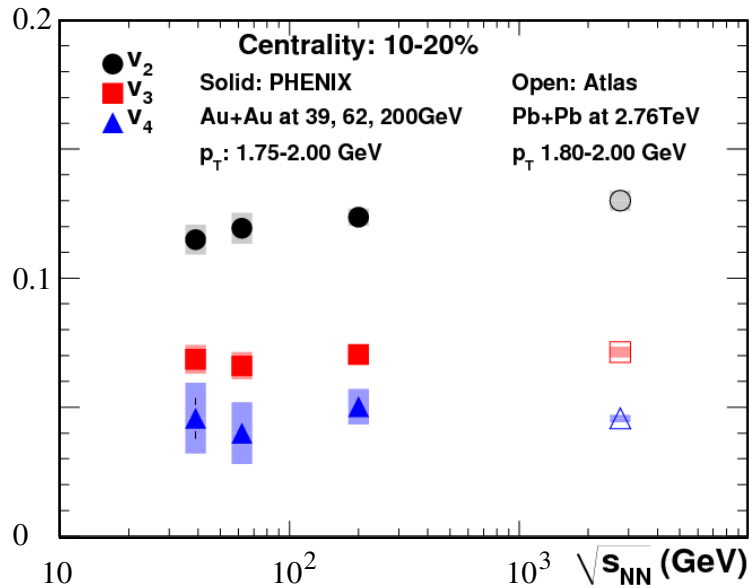


Figure 6: Data for v_{2-4} for collisions of $A + A$ at RHIC and LHC energies.

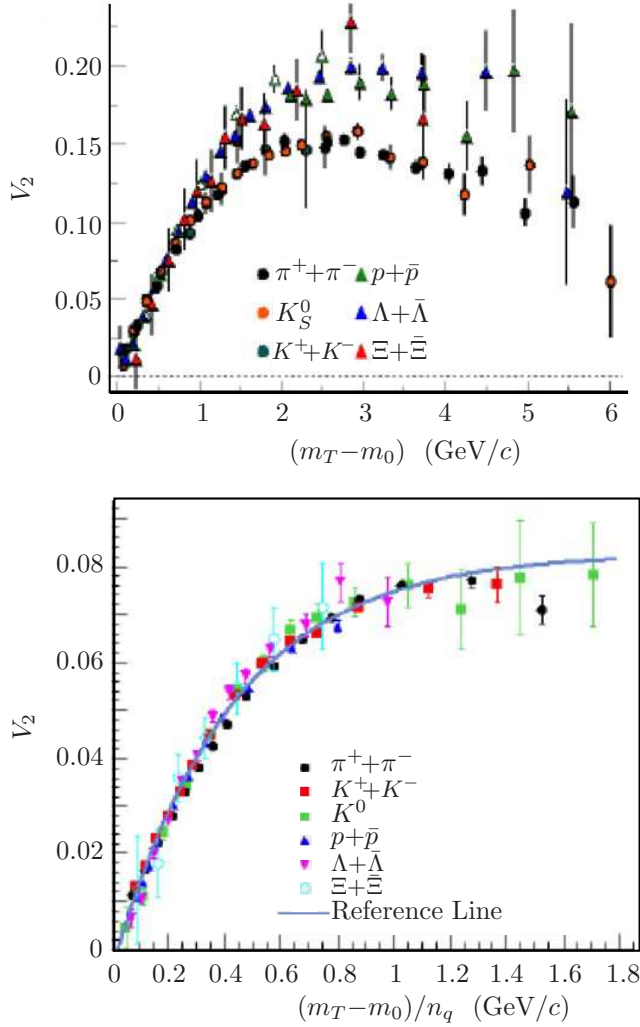


Figure 7: Data for v_2 for baryons and mesons indicating scaling by quark number.

Fluid \rightarrow QuasiParticles \rightarrow Hadrons

and baryons ($n_q = 3$) for 200 GeV/A Au+Au collisions. Note that on the average the v_2 for baryons is higher than for mesons. On the bottom panel we have plotted the same parameters but with each divided by the appropriate quark number n_q . Note that the meson and baryon points come together in a common curve thus scaling according to the valence quark count. The scaling identifies collective behavior as established during the partonic phase of evolution of the system indicating that the degrees of freedom are partonic. This is a direct signature of deconfinement and production of the QGP.

Although the flow has been established for particles containing u , d and s quarks, it is of interest to determine if the much heavier c and b quarks produced in 200 GeV/A Au + Au collisions exhibit flow. In the bottom part of Fig. 4 v_2 is plotted in blue for electrons and positrons from decays of particles with open c and b quarks. For comparison v_2 for π^0 is shown in red. The flow for particles with c and b quarks is

less than for π^0 but is still significant.

The results from the studies of flow at RHIC and LHC can be summarized as follows:

1. The elliptic flow is observed for Au and Pb collisions.
2. The flow at higher energy densities at the LHC is very similar to that at RHIC indicating the saturation.
3. The flow is significant for heavy c and b quarks.
4. The quark scaling of v_2 supports the formation of the QGP.

4 Temperature of the QGP

A primary goal of studies of the sQGP is to measure its temperature through observation of prompt gamma rays emitted as the nuclear fireball expands. The gamma ray spectrum is complex since the photons are emitted in all phases of the expansion. A diagram illustrating this process is shown in Fig. 8. In the initial phase hard scattering of the incident quarks produces jets that emit bremsstrahlung and thermalize producing the sQGP. The plasma next expands into a mixed phase eventually hadronizing into a hadron gas. The phases from sQGP to the hadron gas can be described by relativistic hydrodynamics.

In order to estimate the temperature of hot hadronic matter produced at RHIC, PHENIX measured dilepton production for 200 GeV/A Au and p collisions. These data were used to deduce the direct photon spectra shown in Fig. 9. The figure also shows estimated yields of photons from various stages of the collision. As can be seen from the figure the photon yield becomes softer but more intense as the reaction progresses from the initial hard scattering to the final stages of hadronization.

The data from the PHENIX measured dilepton production for 200 GeV/A Au and p collisions are also shown in Fig. 10. The data are compared with a number of theoretical calculations that assume a system with an initial temperature between 300 and 600 MeV and formation times between 0.6 and 0.15 fm/ c . The PHENIX data are in good agreement with calculations [9] that assume initial temperatures above 300 MeV which is well above the predicted formation temperature for the QGP of 170 MeV.

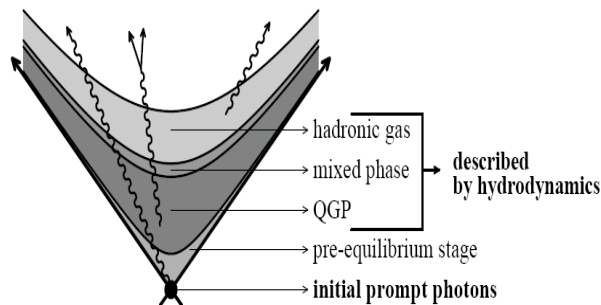


Figure 8: Diagram showing the phases in formation and expansion of the sQGP.

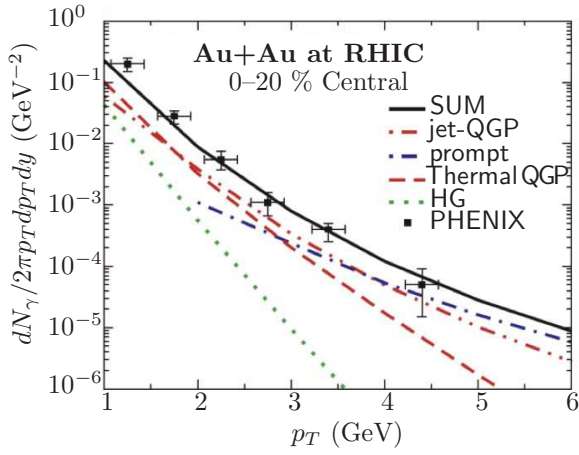


Figure 9: Photon yields from Au + Au collisions compared with calculated yields from various stages of the collision.

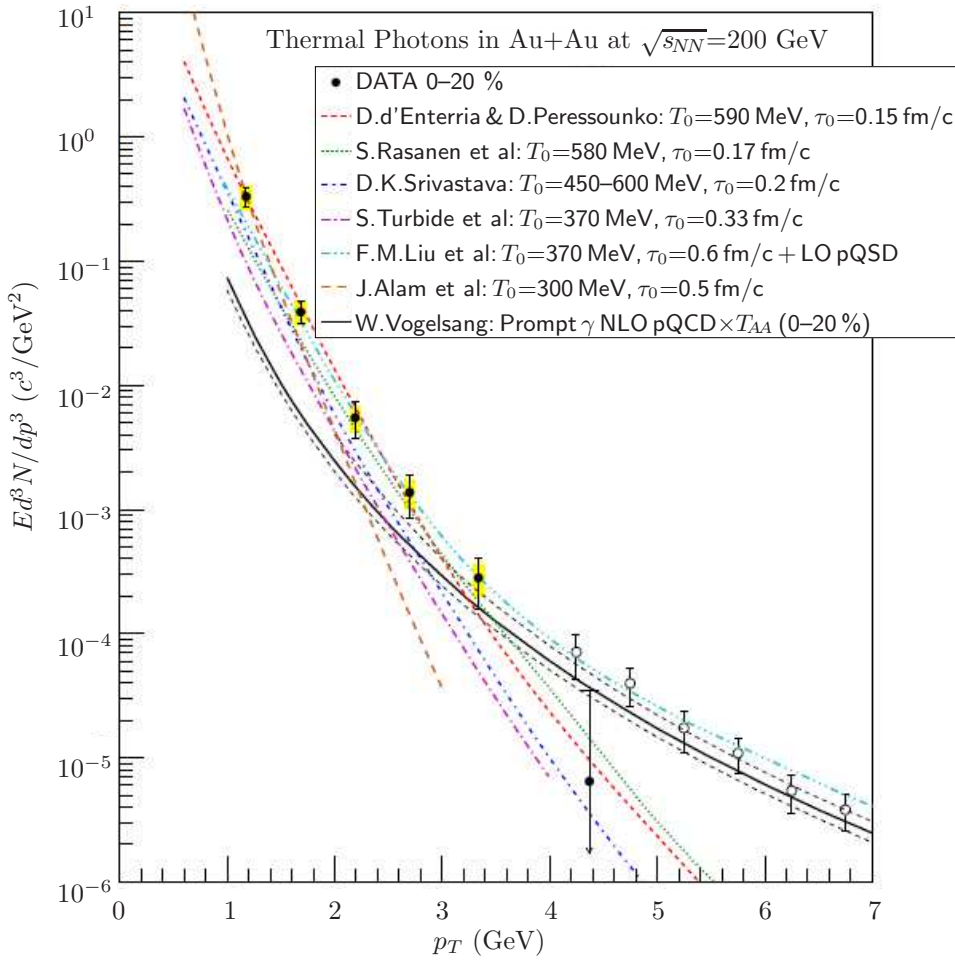


Figure 10: Spectrum of thermal photons from Au + Au collisions at 200 GeV/A compared with calculations assuming various values for formation energies and times.

5 The QGP and long-range correlations in low mass systems

In relativistic $A + A$ collisions a sQGP medium is formed which signals its presence through the long range correlations and a finite flow v_2 . It was thought that $p + p$ and $p + A$ collisions could not form such a medium because of the small system size. Recently results from ALICE [10] and CMS [11] for 5.02 TeV $p + \text{Pb}$ collisions at the LHC indicate the presence of long range correlations. A small v_2 and ridge were observed indicating the long range correlations and a significant flow. One might argue that for the lower beam energies at RHIC such correlations would be absent or much smaller. It is thus of interest to explore whether v_2 and a ridge would be observed with $d + \text{Au}$ collisions at RHIC at 200 GeV/A. In Fig. 11 results for v_2 for 200 GeV $d + \text{Au}$ for the 0 to 5% most central collisions are shown [12] and compared with the results of similar centrality for 5.02 TeV $p + \text{Pb}$ collisions at the LHC [10]. The following observations can be made.

1. A mass splitting of v_2 is seen for both $d + \text{Au}$ and $p + \text{Pb}$ reactions with v_2 generally larger for pions.
2. The viscous hydrodynamics [6] describes $d + \text{Au}$ below $p_T = 2.0 \text{ GeV}/c$.
3. Note a larger mass splitting for $p + \text{Pb}$ below $p_T = 2.0 \text{ GeV}/c$ that may indicate a stronger radial flow for $p + \text{Pb}$.

It is clear from Fig. 11 that a non-zero v_2 and flow are observed for both relativistic $d + \text{Au}$ collisions at RHIC and $p + \text{Pb}$ collisions at the LHC. It is thus of interest to determine if a ridge is observed in $d + \text{Au}$ collisions at RHIC. Therefore a correlation function $C(\Delta\phi, p_T)$ is constructed in the following steps.

1. Correlate one track in the central arm with one in the forward muon piston calorimeter.

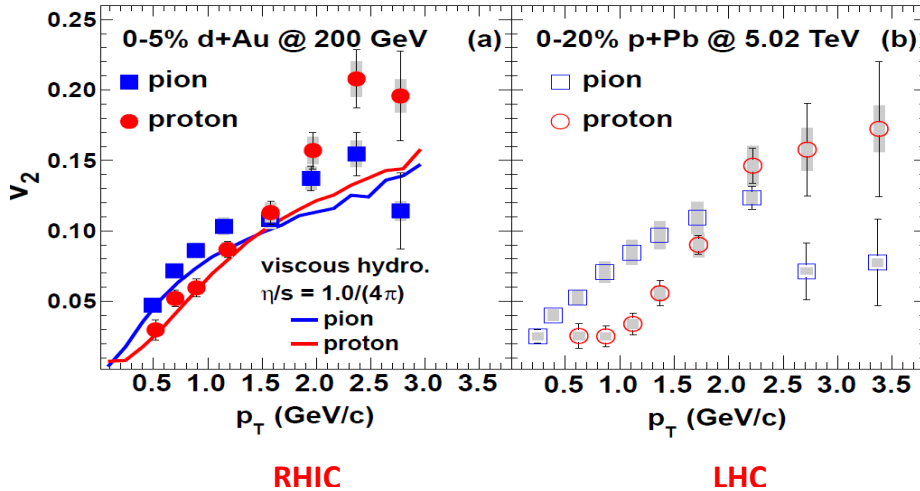


Figure 11: v_2 observed for 200 GeV $d + \text{Au}$ collisions.

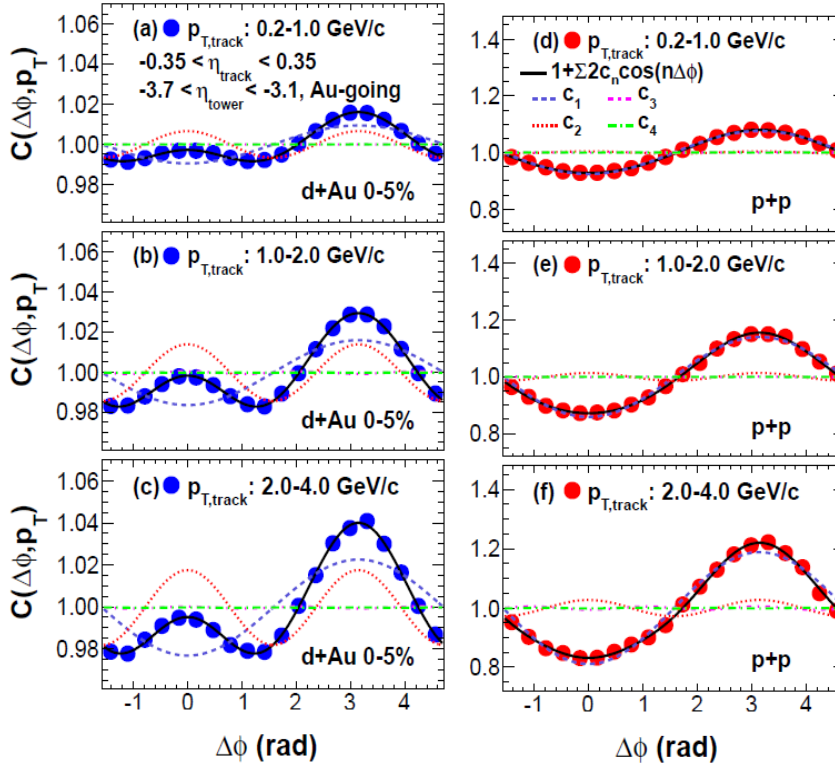


Figure 12: Correlation functions for Au + Au and $p + p$ collisions at RHIC.

2. Construct a signal distribution $S(\Delta\phi, p_T)$ where $\phi = \phi_{track} - \phi_{tower}$.
3. Construct mixed-event distribution $M(\Delta\phi, p_T)$ from different events.
4. Construct a normalized correlation function $C(\Delta\phi, p_T)$.

Correlation functions for central $d + Au$ collisions and mid-bias $p + p$ collisions for several p_T ranges [12] are shown in Fig. 12. Fits from c_1 to c_4 in $\cos(n\Delta\phi)$ are shown. The following conclusions can be drawn.

1. The $p + p$ reactions are dominated by the dipole term (no ridge).
2. The $d + Au$ reactions show a near side peak (ridge) that increases with p_T .

Since the $d + Au$ reactions show a ridge it is of interest to study in more detail the separate correlation functions from the d going and the Au going sides of the reaction. The result of this comparison is shown in Fig. 13. Note that a ridge is clearly visible for the Au but not for the d going side. Also the c_2 component for the d going side is not zero but is much reduced compared to c_2 for the Au going side. Studies of the correlation functions have also been made for the d and Au going sides as a function of centrality. For the Au going side there is a clear ridge that emerges as the centrality is increased. The peripheral collision pattern is similar for the d and Au sides showing essentially no ridge. For the d side no ridge is observed but the c_2 correlation increases with centrality [7].

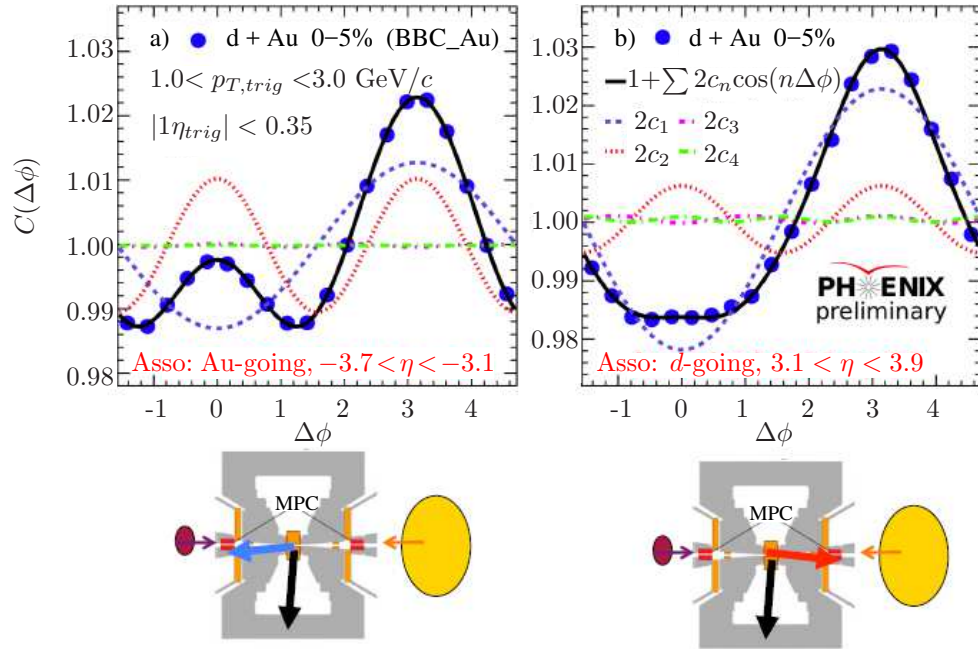


Figure 13: Comparison of correlation functions for the d going and Au going sides of $d + Au$ collisions.

Since long range correlations were observed in $d + Au$ collisions it was of interest to observe if such correlations were present in $^3\text{He} + Au$ collisions. Data was collected

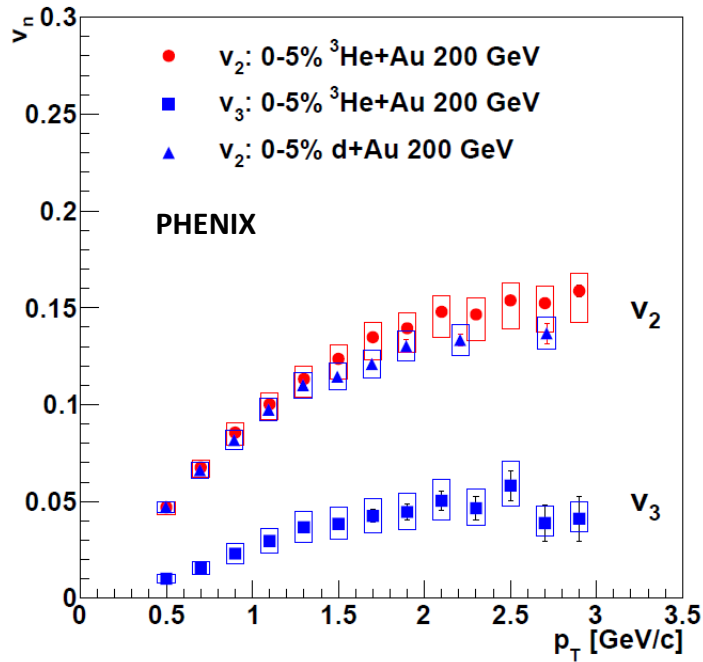


Figure 14: Measured v_2 and v_3 for 0-5% $^3\text{He} + Au$ collisions.

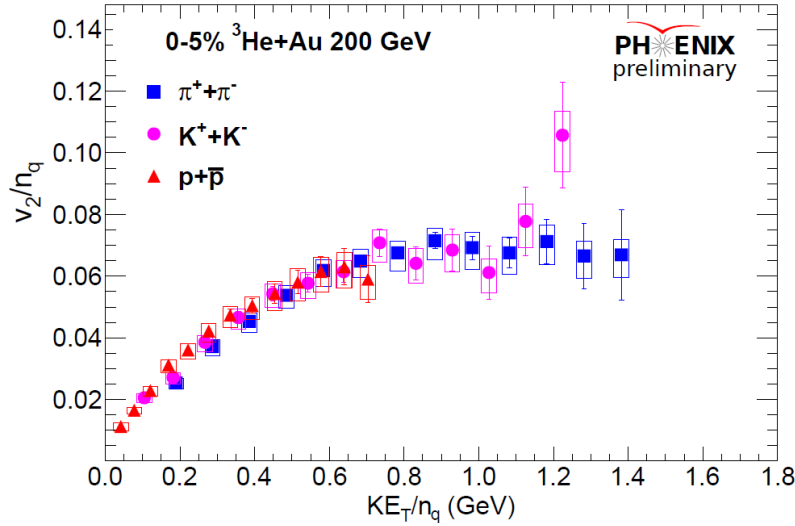


Figure 15: Quark scaling observed in central ${}^3\text{He} + \text{Au}$ collisions.

for ${}^3\text{He} + \text{Au}$ collisions for two weeks at 200 GeV/A at RHIC. A sample of 2.2 billion events at MB was collected. These collisions can be thought of as producing three hot spots that should result in a significant n_3 as well as a n_2 component of flow. A ridge was observed in high multiplicity (0–5%) ${}^3\text{He} + \text{Au}$ collisions. In the reference $p + p$ collisions, the correlation was dominated by momentum conservation (including di-jets). A sizable v_2 and v_3 were observed in 0–5% ${}^3\text{He} + \text{Au}$ collisions [13], extracted by the event plane method as is shown in Fig. 14. The v_2 in 0–5% ${}^3\text{He} + \text{Au}$ and 0–5% $d + \text{Au}$ collisions is very similar [12]. Also a significant v_3 component is observed for the ${}^3\text{He} + \text{Au}$ collisions.

For identified charged particles v_2 was determined for the 0–5% ${}^3\text{He} + \text{Au}$ collisions at 200 GeV/A. Differences in the values for nucleons and mesons was observed at high p_T . This behavior is very similar to that in Au + Au collisions. As can be seen in Fig. 15 mesons and nucleons fall on a smooth curve when each particle v_2 is divided by its n_q . Thus the conclusion is that the quark scaling observed in Au + Au collisions has now been seen in the small ${}^3\text{He} + \text{Au}$ system. Flow and the ridge have been observed for collisions of Au on p , d and ${}^3\text{He}$ at RHIC and $p + \text{Pb}$ at the LHC. This suggests that in some cases QGP droplets have been formed in high energy collisions of large with small nuclei.

6 Results from low energy scans of Au + Au systems

Since the first collisions of Au + Au in the summer of 2000, RHIC has run a number of energy projectile combinations including Au + Au, U + U, Cu + Au, Cu + Cu, ${}^3\text{He} + \text{Au}$, $d + \text{Au}$ and $p + p$. The results from Au + Au collisions can be used to test the beam energy scaling. RHIC has provided Au + Au collision energies of 7.7, 15, 19.6, 27, 39, 62.4, 130 and 200 GeV/A providing a wide range of energies to test the energy scaling. To test the quark scaling, the yields of Au + Au collisions from 7.7 to 200 GeV/A were determined as a function of centrality [14]. The results are

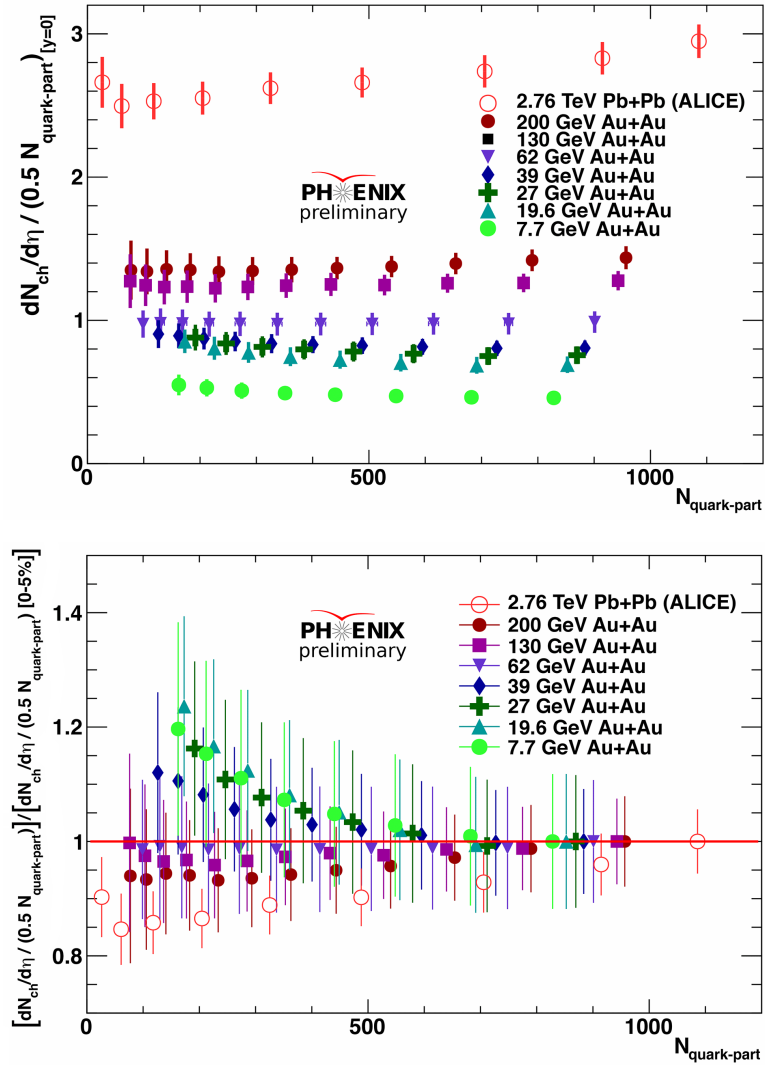


Figure 16: Beam energy scan quark scaling results for Au + Au collisions.

shown in Fig. 16. The plot on the upper panel in the figure shows the yield of Au+Au collisions from 7.7 to 200 GeV/A as a function of centrality but divided by the number of valence quarks. The plot on the lower panel shows the same data but with the highest centrality points for each beam energy normalized to 1.0 to show the trends.

As can be seen from Fig. 16, the quark scaling works well from 200 to 62 GeV but breaks down at lower energies. A plot can also be made (not shown) [14] where the yield is divided by the number of nucleons rather than the number of quarks. That plot shows that the nucleon scaling works well for energies below 40 GeV.

7 Studies of the nuclear fireball radii using the HBT method

In 1956 Hanbury Brown and Twiss (HBT) measured the angular diameter of Sirius from light by observing correlations of light from different parts of the planet's surface [15]. In 1960 Goldhaber *et al.* [16] measured correlation functions between pions in $p+\bar{p}$ reactions. It is thus possible to use HBT to determine correlation functions for the QGP fireball at kinetic freeze out. In order to do this, the 2-particle pion correlation functions of the form $C_2(q) = A(q)/B(q)$ were constructed using the following steps.

1. $A(q)$ is the measured distribution momentum difference $q = p_2 - p_1$.
2. $B(q)$ is the pair uncorrelated distribution from different events.
3. $C_2(q) = N[(\lambda(1 + G(q)))F_c + (\lambda - l)]$.
4. $G(q) = \exp(-R_{side}^2 q_{side}^2 - R_{out}^2 q_{out}^2 - R_{long}^2 q_{long}^2)$.

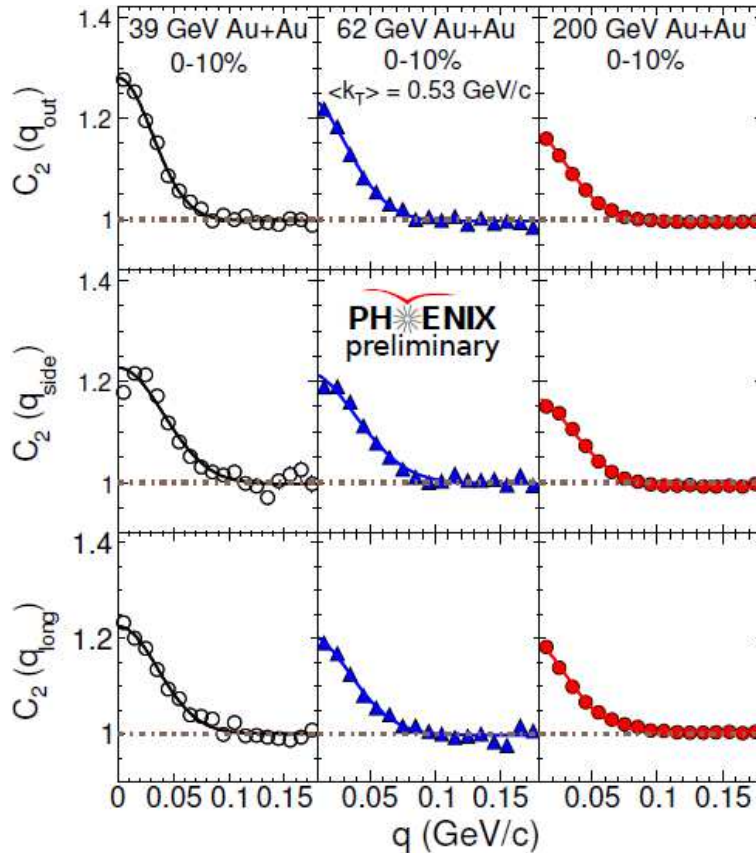


Figure 17: C_2 for 39, 62 and 200 GeV Au + Au central collisions.

In the equations above N is a normalization factor, λ is the correlation strength, F_c is the Coulomb correction factor and the R 's are the measured Gaussian HBT radii. The parameterization of Bertsch [17] and Pratt [18] was used for R where R_{long} is measured in the $q_{long} = 0$ frame. The parameter q_{long} is along the beam direction, q_{out} is parallel to k_T of the pair and q_{side} is perpendicular to the beam and k_T of the pair. The measured $C_2(q)$ can be used to determine R .

The C_2 correlation functions for 39, 62 and 200 GeV collisions of Au + Au [19] are shown in Fig. 17. From the correlation functions $C_2(q_{out})$, $C_2(q_{side})$ and $C_2(q_{long})$ the corresponding HBT pion radii R_{out} , R_{side} and R_{long} were calculated [14]. The radii have interesting scaling properties. Results for radii determined by both STAR [20] and PHENIX [21] are consistent with radii scaling linearly with $m_T^{-1/2}$. In addition it is found that the HBT pion radii scale linearly with the initial radius [19]. These results are consistent with calculations [21] which associate a larger expansion time with a larger size. In Fig. 18 the measured HBT pion radii are plotted as a function of Au + Au collision energy [19]. The results include data from PHENIX, STAR and ALICE. All the data is interpolated to $m_T = 0.26$ GeV. This is valid due to the m_T scaling. For all three radii an increase of kinetic freeze out radius with collision energy is observed.

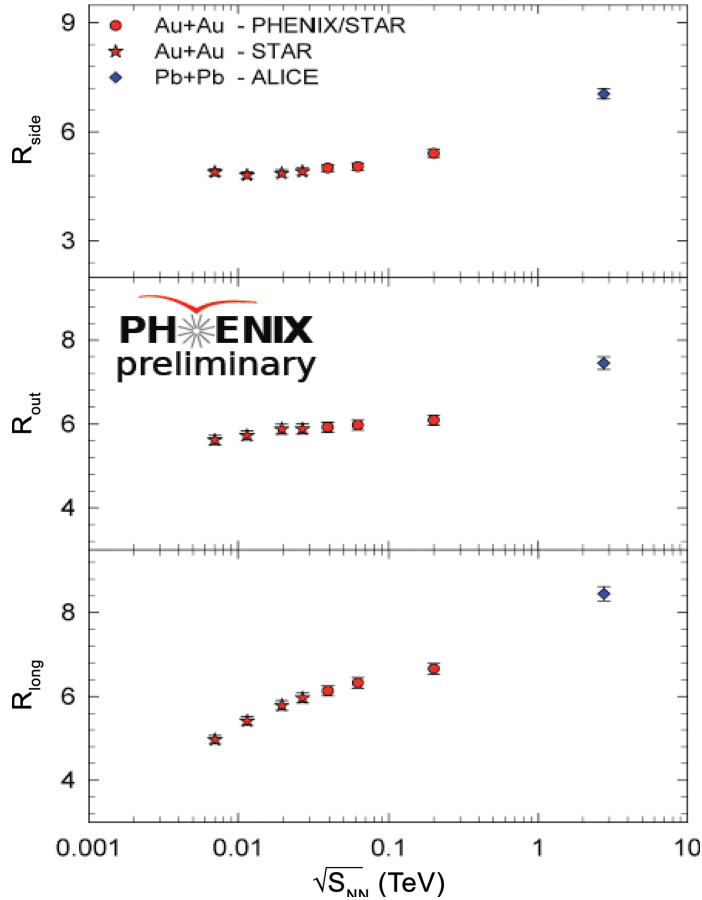


Figure 18: Results for HBT radii vs collision energy.

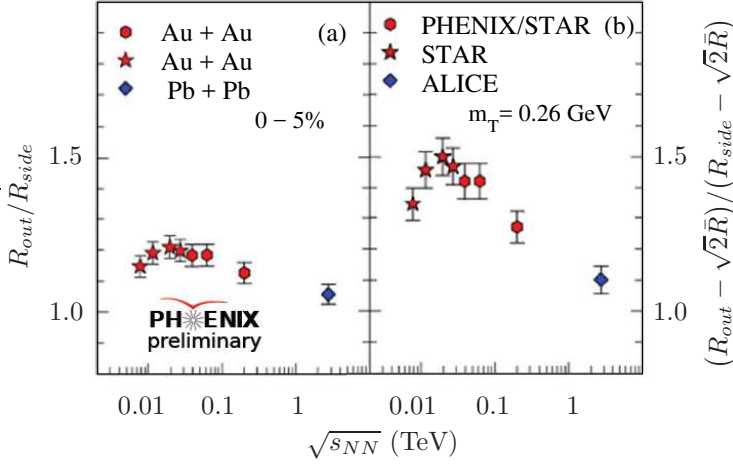


Figure 19: Trends of radii results with energy.

Ratios and differences of various HBT radii give information on both the kinetic freeze out time τ and the duration of kinetic freeze out $\Delta\tau$. $R_{out}^2 - R_{side}^2$ is a proxy for emission duration $\Delta\tau$ and R_{side}/R_{long} is a proxy for expansion speed and the speed of sound c_s in the medium [22]. The results for these parameters as a function of Au + Au collision energy are shown in Fig. 19. The results are not linear with energy. The curve for $R_{out}^2 - R_{side}^2$ shows a maximum in the vicinity of 30 GeV collision energy. The curve for R_{side}/R_{long} shows a minimum in the vicinity of 30 GeV [19]. These non-monotonic patterns are consistent with the minimum observed as a function of collision energy for the viscous coefficients [22] and could be a further indication of trajectories passing through the softest region in the Equation of State (EoS).

8 The future and sPHENIX

The next generation of PHENIX is designated sPHENIX. A primary goal of the sPHENIX program is to complete the picture for the sQGP of its evolution and coupling strength from the initial high temperature through expansion and cooling to the transition scale and below. A fragmentation of partons will be studied by measuring jets and the melting of the three Υ states, namely $1s$, $2s$ and $3s$. The direct photons and high p_T hadrons will be measured with higher statistics than in the past due to high rates and large acceptance expected with sPHENIX. It will be possible to study the R_{AA} of photons, jets, charged mesons and baryons and π^0 s at higher p_T . For example it should be possible to measure direct γ and charged hadrons up to 50 GeV/ c . The detector will be optimized to study jets. It should thus be possible to study jets up to 75 GeV/ c and b jets up to 40 GeV/ c .

An artists view of sPHENIX is shown in Fig. 20. A critical component of the detector was the solenoid magnet acquired from the Babar experiment. The sPHENIX detector is basically cylindrically symmetric. Starting from the interaction point at the center of the detector there is an electromagnetic calorimeter followed by an inner hadronic calorimeter. Next comes the Babar solenoid magnet and finally the outer hadronic calorimeter. Tracking detectors will be located near the beam interaction point.

A major goal for the sPHENIX program will be to study melting of the three Υ

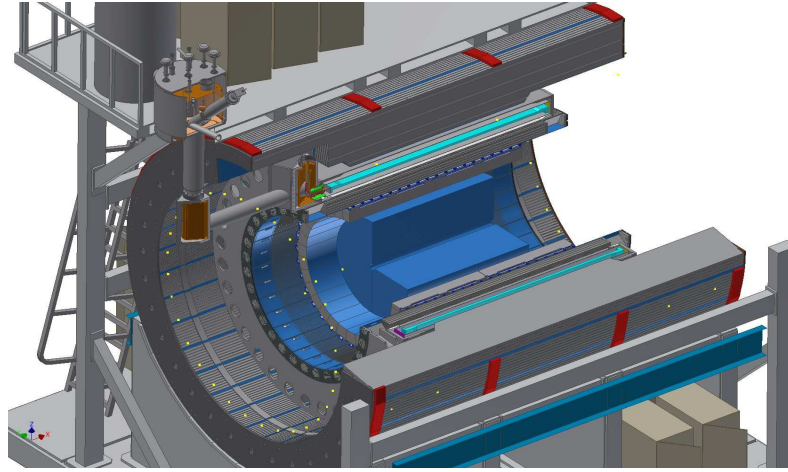
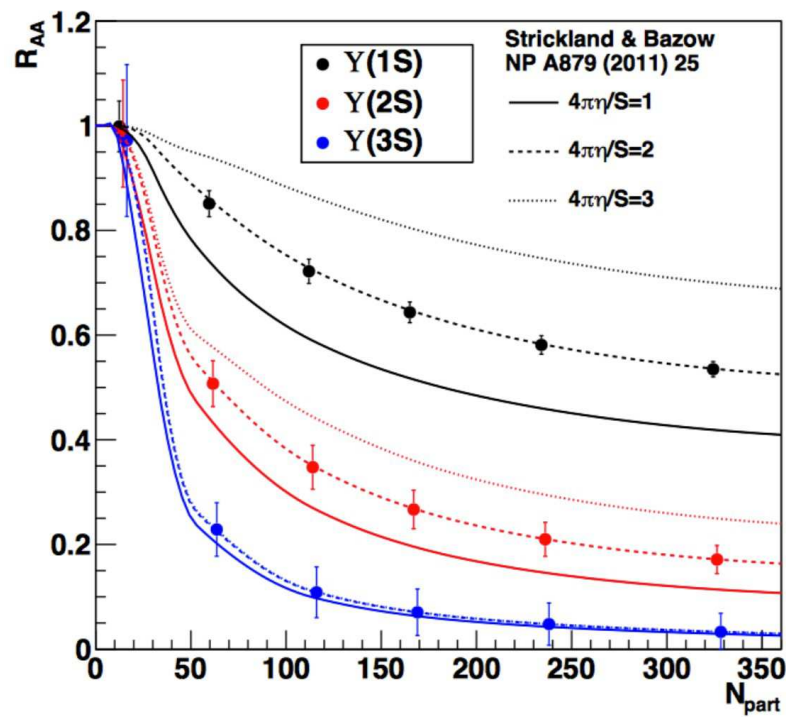


Figure 20: An artist's view of sPHENIX.

states in the sQGP. Figure 21 shows a simulation of R_{AA} data for the three Υ states that could be obtained after 22 weeks of Au + Au and 10 weeks of $p + p$ running. Calculations [16] indicate the relative suppression of the three states. This should give information on the temperature of the sQGP at the point where the melting of the Υ states occurs.

Figure 21: Nuclear modification projections for Υ .

The present status of sPHENIX is as follows. A Department of Energy panel accepted the science case for sPHENIX at a review completed May 2015. Brookhaven National Laboratory (BNL) has made sPHENIX an integral part of its plan for the future now that the PHENIX experiment has been completed in 2016. Design, simulation, R&D, and prototyping for sPHENIX are all moving forward. BNL convened a workshop to form a new sPHENIX collaboration in June 2015 and the first collaboration meeting was held on December 10–12, 2015 at Rutgers University. The planning calls for the sPHENIX detector to begin operation in 2022.

9 Conclusions

The main conclusions from the above paper are listed below:

1. A hot dense medium has been created in Au + Au collisions. The evidence is a nuclear modification factor $R_{AA} < 1.0$.
2. The hot dense medium flows. The sQGP acts as a high temperature low viscosity liquid. The evidence is $v_2 > 0$.
3. The sQGP is actually created. The evidence is the quark scaling of v_2 for mesons ($q = 2$) and baryons ($q = 3$).
4. No phase transition is observed implying the crossover from the sQGP to a hadron gas.
5. The evidence for QGP droplets is observed in p , d and ^3He collisions with heavy nuclei.
6. HBT studies measured radii at freeze out and point to a possible softening of the nuclear EoS around 30 GeV.
7. The predicted first order phase transition and critical point yet to be observed.
8. The PHENIX program ended in 2016 and now the collaboration is transitioning to sPHENIX.

References

- [1] K. Adcox *et al.*, Nucl. Phys. A **757**, 184 (2005).
- [2] A. Adare *et al.*, Phys. Rev. Lett. **101**, 232301 (2008).
- [3] A. Adare *et al.*, Phys. Rev. C **82**, 011902 (2010).
- [4] A. Adare *et al.*, Phys. Rev. C **84**, 044902 (2011).
- [5] A. Adare *et al.*, Phys. Rev. C **83**, 024909 (2011).
- [6] S. Afanasiev *et al.*, Phys. Rev. Lett. **109**, 152302 (2012).
- [7] A. Adare *et al.*, Phys. Rev. Lett. **109**, 152301 (2012).
- [8] J. Adams *et al.*, Phys. Rev. C **72**, 014904 (2005).

- [9] P. Huovinen, private communication (2004).
- [10] B. Abelev *et al.* (ALICE Collaboration), Phys. Lett. **B726**, 164 (2013).
- [11] D. Abbaneo *et al.* (CMS Collaboration), Phys. Lett. **B718**, 795 (2013).
- [12] A. Adare *et al.* (PHENIX Collaboration), Phys. Rev. Lett. **114**, 192301 (2015).
- [13] A. Adare *et al.* (PHENIX Collaboration), Phys. Rev. Lett. **115**, 142301 (2015).
- [14] R. Soltz (for the PHENIX Collaboration), Nucl. Phys. A **931**, 780 (2014).
- [15] R. H. Brown and R. Q. Twiss, Nature **178**, 1046 (1956).
- [16] G. Goldhaber, S. Goldhaber, W. Lee and A. Pais, Phys. Rev. **120**, 300 (1960).
- [17] G. Bertsch, Nucl. Phys. A **498**, 173 (1989).
- [18] S. Pratt, Phys. Rev. D **33**, 1314 (1986).
- [19] A. Adare *et al.* (PHENIX Collaboration), arXiv:1410.2559 (2014).
- [20] L. Adamczyk *et al.* (STAR Collaboration), Phys. Rev. C **92**, 014904 (2015).
- [21] E. Shuryak and I. Zahed, Phys. Rev. C **88**, 044915 (2013).
- [22] R. A. Lacey, A. Taranenko, J. Jia, D. Reynolds, N. N. Ajitanand, J. M. Alexander, Y. Gu and A. Mwai, Phys. Rev. Lett. **112**, 082302 (2014).